*Processes* **2015**, *3*, 50-70; doi:10.3390/pr3010050

OPEN ACCESS

*processes*

**ISSN 2227-9717**

www.mdpi.com/journal/processes

*Article*

# Modeling the Dynamics of Acute Phase Protein Expression in Human Hepatoma Cells Stimulated by IL-6

**Zhaobin Xu [1], Jens O. M. Karlsson [2] and Zuyi Huang [1,3,4,*]**

[1] Department of Chemical Engineering, Villanova University, Villanova, PA 19085, USA; E-Mail: zxu2@villanova.edu

[2] Department of Mechanical Engineering, Villanova University, Villanova, PA 19085, USA; E-Mail: jens.karlsson@villanova.edu

[3] The Center for Nonlinear Dynamics& Control (CENDAC), Villanova University, Villanova, PA 19085, USA

[4] The Villanova Center for the Advancement of Sustainability in Engineering (VCASE), Villanova University, Villanova, PA 19085, USA

* Author to whom correspondence should be addressed; E-Mail: zuyi.huang@villanova.edu; Tel.: +1-610-519-4848; Fax: +1-610-519-7354.

Academic Editor: Juergen Hahn

*Received: 22 August 2014 / Accepted: 9 December 2014 / Published: 14 January 2015*

---

**Abstract:** Interleukin-6 (IL-6) is a systemic inflammatory mediator that triggers the human body's acute phase response to trauma or inflammation. Although mathematical models for IL-6 signaling pathways have previously been developed, reactions that describe the expression of acute phase proteins were not included. To address this deficiency, a recent model of IL-6 signaling was extended to predict the dynamics of acute phase protein expression in IL-6-stimulated HepG2 cells (a human hepatoma cell line). This included reactions that describe the regulation of haptoglobin, fibrinogen, and albumin secretion by nuclear transcription factors STAT3 dimer and C/EBPβ. This new extended model was validated against two different sets of experimental data. Using the validated model, a sensitivity analysis was performed to identify seven potential drug targets to regulate the secretion of haptoglobin, fibrinogen, and albumin. The drug-target binding kinetics for these seven targets was then integrated with the IL-6 kinetic model to rank them based upon the influence of their pairing with drugs on acute phase protein dynamics. It was found that gp80, JAK, and gp130 were the three most promising drug targets and that it

was possible to reduce the therapeutic dosage by combining drugs aimed at the top three targets in a cocktail. These findings suggest hypotheses for further experimental investigation.

**Keywords:** systems engineering; cellular biology and engineering; kinetics; mathematical modeling; parameter estimation; sensitivity analysis

## 1. Introduction

Interleukin-6 (IL-6) has been identified as one of the major systemic mediators that orchestrate acute phase response (APR) in the human body, as evidenced by the fact that IL-6 can stimulate the synthesis of most acute phase proteins in liver cells [1]. The mediation of APR by IL-6 begins with the release of IL-6 by leukocytes at the injury site. IL-6 then translocates to the liver, via the blood stream, where it stimulates hepatocytes and activates a cascade of intracellular signal transduction pathways. This leads to the activation of transcription factors, such as nuclear STAT3 dimer and C/EBPβ. These transcription factors, in turn, regulate the expression of acute phase proteins, such as haptoglobin, fibrinogen and albumin. The IL-6 signal transduction pathway has been extensively studied and the two major signaling pathways have been determined to be the JAK-STAT pathway and the MAPK-C/EBPβ pathway [2]. Nuclear STAT3 dimer and C/EBPβ have been identified as the transcription factors involved in these two signaling pathways, respectively [3,4]. Mathematical models have been developed for the JAK-STAT pathway [5] and the MAPK pathway [6–8]. Singh *et al.* (2006) presented the first comprehensive mathematical model for the IL-6 signal transduction pathway by integrating models for both the JAK-STAT and the MAPK pathways [9]. Moya *et al.* (2011) further extended the model of the MAPK pathway to predict the activation dynamics of transcription factor C/EBPβ [10]. However, acute phase proteins, which represent the end products of the IL-6 signal transduction pathway and participate in the human body's response to trauma or inflammation, were not included in these existing mathematical models. Ryll *et al.* (2011) presented the first attempt to incorporate expression of acute phase proteins (e.g., C-reactive protein, α2-macroglobulin, and fibrinogen) in a model of the IL-6 signaling network [11]. However, this was a qualitative logic model in which the detailed intermediate reactions for acute phase protein activation were neglected. To address this deficiency, the model presented by Moya *et al.* (2011) [10] will be extended in this work to predict the dynamics of acute phase protein expression in HepG2 cells. Haptoglobin, fibrinogen, and albumin were selected as the representative acute phase proteins in this work for model development. These were chosen because they represent both positive (*i.e.*, haptoglobin and fibrinogen) and negative (*i.e.*, albumin) acute phase proteins and quantitative experimental data for the expression dynamics of these three proteins in HepG2 cells stimulated by IL-6 were available in the literature [12].

Mathematical models have previously been developed, and used, to identify potential drug targets to treat human diseases. For example, Araujo *et al.* (2005) presented a modeling approach to study the effect of multiple drugs on EGFR signaling [13]. Yang *et al.* (2008) further extended Araujo's approach to determine multiple-target optimal intervention in the arachidonic acid metabolic network [14]. Such model-based approaches require that equations describing the signaling kinetics be integrated with models of target-drug binding kinetics. Since there is a lack of models of acute phase protein

expression and limited information about relevant target-drug binding kinetics in the IL-6 pathway, model-based approaches have not previously been applied to the identification of drug targets for regulating the dynamics of acute phase proteins stimulated by IL-6. In order to address this, our extended IL-6 model will be used in a sensitivity analysis to identify potential drug targets for regulating the expression dynamics of albumin, haptoglobin, and fibrinogen. Targeting JAK kinases could be useful in the treatment of a variety of diseases, including rheumatoid arthritis (RA) [15], myeloproliferative disorders [16] and cancers [17]. The approved pan-JAK inhibitor, tofacitinib, has undergone extensive evaluation for RA and has demonstrated efficacy in various clinical trials, likely due to its suppression of the IL-6 and cytokine pathways [18]. Along with tofacitinib, a series of JAK inhibitors have been proposed recently using a novel fused triazolo-pyrrolopyridine scaffold [18]. Among them is imidazo-pyrrolopyridine. Since limited information is available for drugs that bind to targets other than JAK kinases in IL-6 signaling, this work focuses on JAK inhibitors only. Imidazo-pyrrolopyridine is used as the model drug to illustrate the approach developed to integrate the extended IL-6 model with target-drug binding kinetics for studying the effectiveness of single/multiple drug treatment in regulating the secretion of acute phase response proteins.

This paper is structured as follows: A recent model of IL-6 signaling [10] is extended, in Section 2, to predict the dynamics of acute phase protein expression. Experimental data presented in [12] are used to estimate the unknown model parameters, and the extended model is then validated against independent experimental data reported by [12] and [1]. Based upon the model developed in Section 2, sensitivity analysis is conducted, in Section 3, to identify reactions that play an important role in the regulation of the dynamics of haptoglobin, fibrinogen, and albumin. Molecular components involved in these reactions are regarded as potential drug targets. A model-based approach for virtual drug target screening is presented in Section 4 to evaluate the influence of the interaction between potential drugs and targets on the secretion rate of acute phase proteins. Discussion and concluding remarks related to the obtained results are given in Sections 5 and 6 respectively.

## 2. Model Development for the Kinetics of Acute Phase Proteins in IL-6 Stimulated Hepatocytes

### *2.1. IL-6 Signal Transduction Model*

The starting point for the model used in this work is the IL-6 signal transduction model developed by one of the co-authors (ZH) as described in a previous study [10]. This model can be represented by a set of nonlinear ordinary differential equations (Equation (1)):

$$\frac{d\mathbf{x}}{dt} = f(\mathbf{x}, \mathbf{p}, u) \tag{1}$$

where $\mathbf{x}$ is a vector of the state variables of the model, $\mathbf{p}$ is a vector of the parameters, and $u$ is the input to the system. The model consists of 68 ordinary differential equations representing the mass balances of the individual proteins and protein complexes, 117 parameters describing reaction constants, and one input given by the extracellular IL-6 concentration.

A simplified diagram of the proteins involved in the model is shown in Figure 1. Extracellular cytokine IL-6 initiates the APR by attaching to its receptor at the cell membrane and forming $(IL6\text{-}gp80\text{-}gp130\text{-}JAK)_2$ complex. This phosphorylated dimer serves as the starting point for both the

JAK-STAT and the MAPK pathways. In the JAK-STAT signaling, the phosphorylated dimer recruits the transcription factor STAT3, which is also tyrosine phosphorylated. The phosphorylated STAT3 dissociates from the receptor complex $(IL6\text{-}gp80\text{-}gp130\text{-}JAK)_2$ and undergoes dimerization. The dimerized STAT3 complex translocates to the nucleus and functions as a transcription factor for the expression of SOCS3, which in turn binds to the receptor gp130 and blocks the activation of JAK, thus inhibiting both STAT3 activation and MAPK activation. In the MAPK signaling, phosphorylated gp130 recruits SHP2 which subsequently undergoes phosphorylation. The phosphorylated SHP2 interacts with Grb2 and SOS. The binding of Grb2 and SOS to the receptor complex leads to the activation of RAS, which further leads to the activation of the MAPK cascade up to transcription factor C/EBPβ.

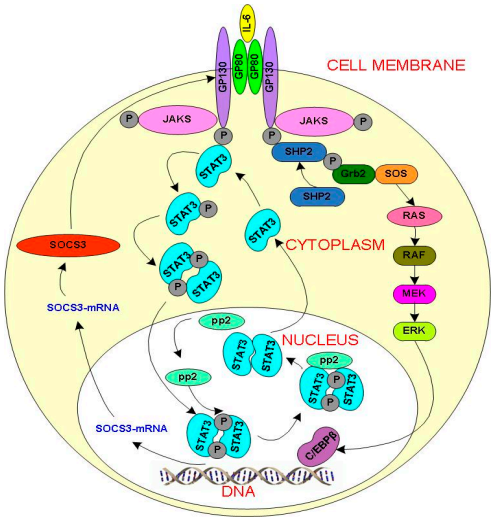


**Figure 1.** Implemented reaction network for Interleukin-6 (IL-6) induced signal transduction in hepatocytes. Adapted with permission from [10]. Copyright 2011, IET.

In this work, the model reported by [10] is extended to predict the expression dynamics of haptoglobin, fibrinogen, and albumin in HepG2 cells stimulated by IL-6. Reactions for the synthesis of haptoglobin, fibrinogen, and albumin are first added into Moya's model. The unknown parameters in the extended model are estimated from the experimental data measured in HepG2 cells under constant exposure to 2 nM IL-6 for seven days [12]. The extended model is then validated by the two data sets: the first one is for HepG2 cells under a pulse-chase stimulation of IL-6 [12], while the second one is for steady state values of dose-dependent secretion rates of fibrinogen and albumin in IL-6-stimulated HepG2 cultures reported by [1].

### *2.2. Extended Model of Acute Phase Protein Expression Dynamics*

The model reported by [10] does not include reactions for the synthesis of haptoglobin, fibrinogen, and albumin. In this subsection, reactions describing the transcription of mRNA encoding haptoglobin, fibrinogen, and albumin, as well as reactions responsible for the translation and secretion of these three acute phase proteins, were added into the existing model of IL-6 signal transduction. Nuclear STAT3 dimer and C/EBPβ, whose activation levels can be regulated by IL-6 signaling, are the two major transcription factors for initiating the expression of acute phase proteins in the liver. In particular, C/EBPβ, nuclear STAT3 dimer, and C/EBPα are the transcription factors regulating the transcription

of haptoglobin [19], fibrinogen [20], and albumin [19,21], respectively. The transcription factor C/EBPβ affects the expression dynamics of albumin by inhibiting the expression of C/EBPα [21], and thus C/EBPβ indirectly down-regulates the expression of albumin. Based on these observations, reactions shown in Equations (2) through (9) were added into the IL-6 model reported by [10] such that the secretion rates of extracellular haptoglobin, fibrinogen, and albumin (denoted as Ex-haptoglobin, Ex-fibrinogen, and Ex-albumin, respectively) can be predicted from the extended model.

$$\mathrm{C/EBP\beta} \xrightarrow{V_{m\_h},K_{m\_h}} \mathrm{mRNA-haptoglobin} \tag{2}$$

$$\mathrm{mRNA-haptoglobin} \xrightarrow{k_{t\_h}} \mathrm{Ex-haptoglobin} \tag{3}$$

$$\mathrm{STAT3N^{*}-STAT3N^{*}} \xrightarrow{V_{m\_f},K_{m\_f}} \mathrm{mRNA-fibrinogen} \tag{4}$$

$$\mathrm{mRNA-fibrinogen} \xrightarrow{k_{t\_f}} \mathrm{Ex-fibrinogen} \tag{5}$$

$$\mathrm{C/EBP\beta} \xrightarrow{k_{i\_a}} \mathrm{C/EBP\alpha} \tag{6}$$

$$\mathrm{C/EBP\alpha} \xrightarrow{k_{d\_a}} \mathrm{degradation} \tag{7}$$

$$\mathrm{C/EBP\alpha} \xrightarrow{V_{m\_a},K_{m\_a}} \mathrm{mRNA-albumin} \tag{8}$$

$$\mathrm{mRNA-albumin} \xrightarrow{k_{t\_a}} \mathrm{Ex-albumin} \tag{9}$$

In Equations (2)–(9), the species mRNA-haptoglobin, mRNA-fibrinogen and mRNA-albumin refer to the mRNA encoding for the corresponding protein. Equation (2) describes the transcription process of haptoglobin, which is regulated by C/EBPβ [19] (the corresponding Michaelis-Menten coefficients are $V_{m\_h}$ and $K_{m\_h}$). Equation (3) lumps the translation of the haptoglobin mRNA with the secretion process of synthesized haptoglobin. Lumping was performed to reduce the number of unknown parameters in the model, and is justifiable since one of the two sequential processes is rate-limiting. Thus, a mass action kinetic model with an effective rate constant $k_{t\_h}$ was used to describe the lumped translation and secretion processes for haptoglobin expression. Similarly, Equations (4) and (5) describe the transcription, translation, and secretion processes of fibrinogen. Compared to these two positive acute phase proteins, the regulation of the expression of albumin, given by Equations (6) to (9), is more complicated. C/EBPβ inhibits the activation of C/EBPα as given in Equation (6). This down-regulates the expression of albumin, because C/EBPα is required to initiate the transcription of albumin (as shown in Equation (8)). Equation (7) describes the degradation process of C/EBPα in HepG2 cells due to the cell growth, while Equation (9) represents the lumped translation and secretion of albumin. A one-day delay has been added in the albumin transcription process as suggested by the data presented in [12]. Figure 2 shows the schematic diagram of the extended IL-6 signal transduction pathway.

The ordinary differential equations describing the rates of newly added components involved in Equations (2) through (9) are developed based on mass balance, mass action kinetics and Michaelis-Menten kinetics. The resulting seven equations, Equations (A1)–(A7) (given in the Appendix), were integrated into our existing IL-6 model [10] to yield an extended IL-6 model with 75 ordinary

differential equations and 128 parameters, to predict the secretion rates of extracellular haptoglobin, fibrinogen, and albumin.

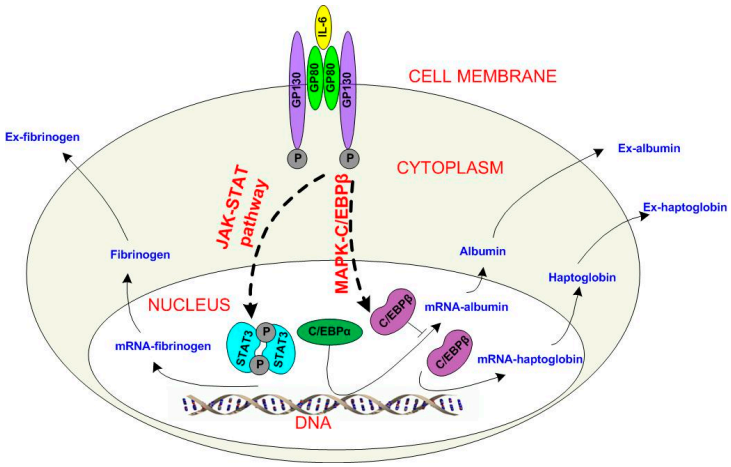


**Figure 2.** Extension of an existing Interleukin-6 (IL-6) signal transduction model [10] to include reactions describing the expression dynamics of haptoglobin, fibrinogen, and albumin. The two dashed lines represent the JAK-STAT and MAPK-C/EBPβ pathways (see Figure 1). Adapted with permission from [10]. Copyright 2011, IET.

### *2.3. Estimation of Unknown Parameters in the Extended Model*

There are 11 unknown parameters in Equations (2) through (9). Fisher information matrixes (FIM) were used to perform identifiability analysis. All these parameters are identifiable. An experimental data set for HepG2 cultures under a seven-day exposure to 2 nM IL-6 [12] was used to estimate these unknown parameters. Parameter estimation was conducted with standard nonlinear least squares optimization routines, such as lsqnonlin, available from MATLAB (The Math Works: Natick, MA, USA). The estimated values of the 11 unknown parameters, as well as their bounds with a 95% confidence level, were listed in the Appendix. A comparison between the model output and the experimental data was shown in Figure 3. In addition to performing comparison by visual inspection, the relative errors (*Err*) were computed according to the Equation (10);

$$Err = \frac{\left\| \mathbf{Y} - \hat{\mathbf{Y}} \right\|}{\left\| \hat{\mathbf{Y}} \right\|} \times 100\% \tag{10}$$

where $\hat{\mathbf{Y}}$ is a vector of the experimentally measured outputs at different points in time, *i.e.*, $\left[\hat{y}(t_1) \quad \hat{y}(t_2) \quad \cdots \quad \hat{y}(t_n)\right]$, and $\mathbf{Y}$ is a vector of the outputs calculated by the model at corresponding time points, *i.e.*, $\left[y(t_1) \quad y(t_2) \quad \cdots \quad y(t_n)\right]$. The norm is the Euclidean ($\ell_2$) norm. The values of *Err* for the secretion rates of haptoglobin, fibrinogen, and albumin were found to be 14.41%, 12.16%, and 7.17%, respectively. All of relative errors were below 15%, which indicates that the prediction was reasonably good in comparison to the magnitude of the error bars in the experimental data.

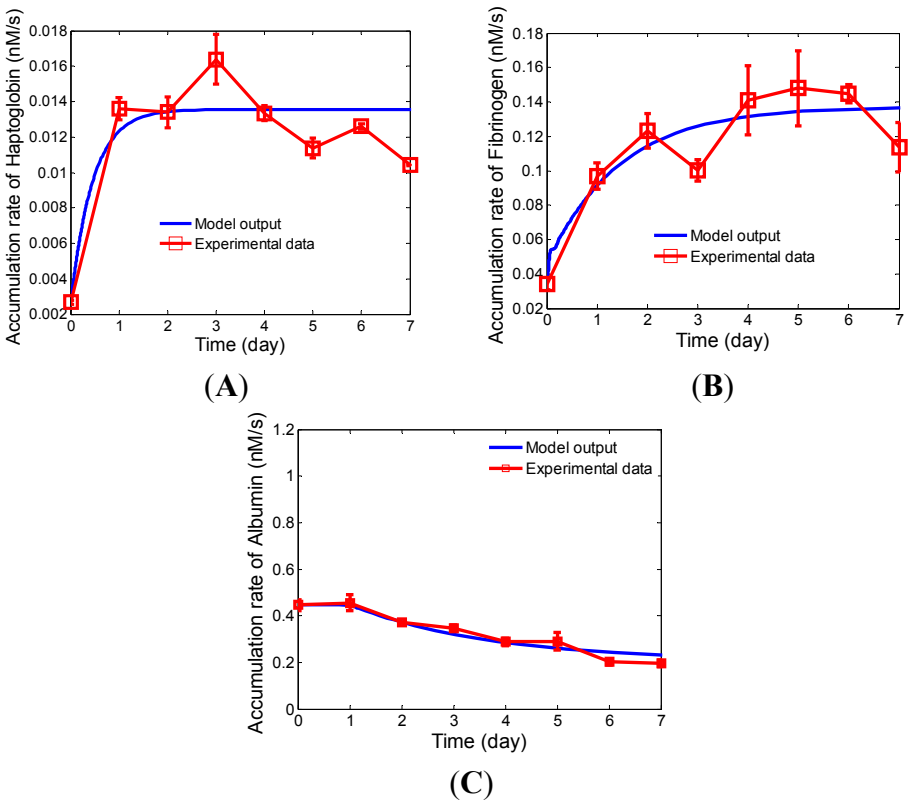


**Figure 3.** Comparison of model-predicted secretion rates of haptoglobin, fibrinogen, and albumin to experimental data obtained from the HepG2 cultures stimulated daily by 2 nM Interleukin-6 (IL-6): (**A**) the secretion rate of haptoglobin; (**B**) the secretion rate of fibrinogen; (**C**) the secretion rate of albumin.

### *2.4. Validation of the Developed Model*

Validation of the developed model is a crucial step before it is used to generate potential biological hypotheses that are used for biological experiment design. In this subsection, two independent experimental data sets were used to verify the developed model.

#### 2.4.1. Relaxation Kinetics of Albumin, Fibrinogen, and Haptoglobin in HepG2 Cultures under a Pulse-Chase Stimulation of IL-6

The developed model was used to predict the dynamics of the three acute phase proteins for a pulse-chase condition where HepG2 cultures were subjected to IL-6 stimulation for three days and thereafter maintained without IL-6 stimulation [12]. Figure 4 showed the comparison between the model prediction and the experimental data. The values of *Err* for the prediction of secretion rates of haptoglobin, fibrinogen, and albumin were 14.78%, 31.09%, and 5.15%, respectively. It can be seen from Figure 4A that the model predicted the relaxation kinetics of haptoglobin well. A large value of *Err* existed in the prediction of relaxation kinetics of fibrinogen. This is mainly due to the mismatch between the model prediction and experimental data in Day two described in Figure 4B, for which the error bar, *i.e.*, the variability of experimental measurements, was quite large. Corresponding explanation for this large error bar has been given in the original report by [12]. Other than Day two, the model prediction for fibrinogen secretion rate matched the experimental data well. The predicted

albumin secretion kinetics agreed well with the experimental data, as shown in Figure 4C, although it was necessary to incorporate a 24 h time-delay in the albumin expression model in order to accurately describe the observed lag between changes in IL-6 concentration and the resulting albumin secretion rate.

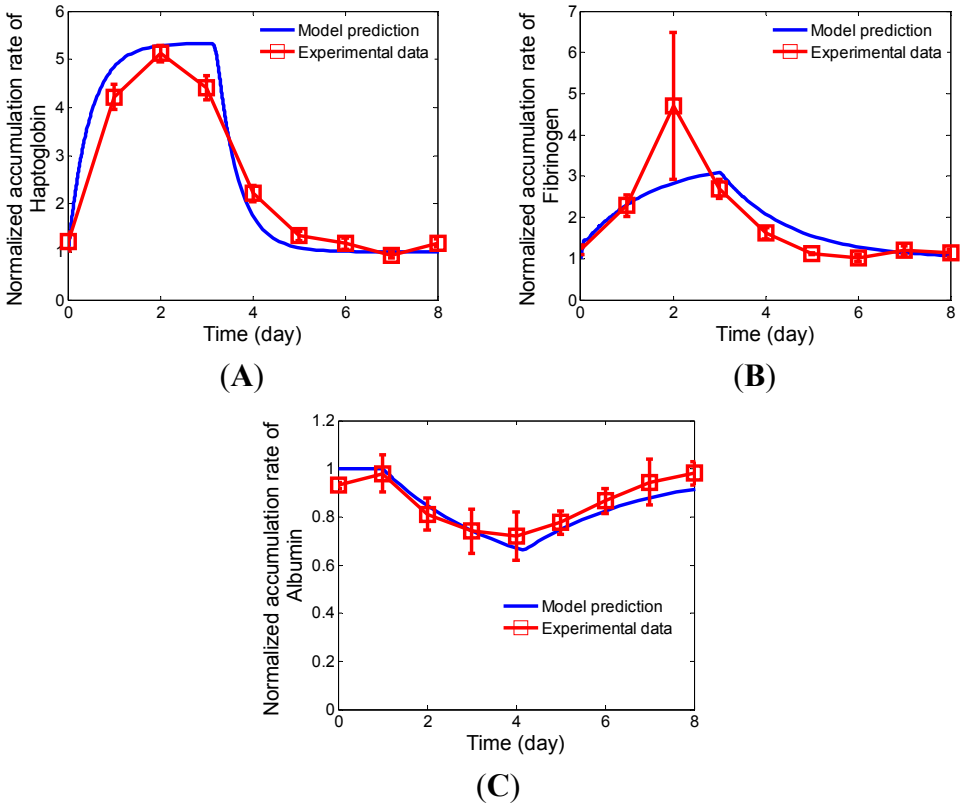


**Figure 4.** Comparison of model prediction to experimental secretion rates of haptoglobin, fibrinogen, and albumin for HepG2 cells under a pulse-chase stimulation of 2 nM Interleukin-6 (IL-6): (**A**) secretion rate of haptoglobin; (**B**) secretion rate of fibrinogen; (**C**) secretion rate of albumin.

### 2.4.2. Steady State Values of Dose-Dependent Secretion Rates of Fibrinogen and Albumin in IL-6 Stimulated HepG2 Cultures

In this subsection, the data published in [1], which includes the steady state secretion rates of fibrinogen and albumin obtained in human primary hepatocytes under the exposure to IL-6 of various concentrations, was used to further validate the extended model. Accordingly, different concentrations of IL-6 were used in this work as the inputs for the developed model, and the steady state values of the secretion rates of fibrinogen, albumin and haptoglobin were recorded, normalized by the secretion rates of these three proteins for the control condition, and plotted in Figure 5. Figure 5A showed that the steady state value of the secretion rate of fibrinogen increased with increasing IL-6 concentrations and leveled off afterwards, following a sigmoidal profile with a transition width corresponding to two orders of magnitude variation in the IL-6 concentration. In addition, the maximum steady-state secretion rate was approximately four-fold higher than for the control condition. Both of these predictions (magnitude and width of profile) were consistent with the corresponding characteristics of the dose-dependence profile reported by [1] for fibrinogen secretion. Figure 5B showed that the

predicted steady-state albumin secretion rate decreased approximately two-fold as the IL-6 concentration increased. The experimental dose response data, measured by [1] for albumin secretion, exhibited an inhibition of similar magnitude (~2.5-fold). However, the width of the transition in the predicted dose response for albumin was narrower than the transition width reported by [1] for this negative acute phase protein. As seen in Figure 5C, the steady-state haptoglobin secretion rates for various IL-6 concentrations followed a similar trend as shown in Figure 5A for steady-state fibrinogen secretion rates, but with a narrower transition width and a higher enhancement in the maximum steady-state secretion rate (around 5 times of the secretion rate for the control condition). Although Heinrich *et al*. [1] did not report the steady-state secretion rates of haptoglobin as a function of IL-6 concentration, the result shown in Figure 5C was generally consistent with the response expected for a positive acute phase. One interesting observation that was made in Figure 5 was that the $ED_{50}$ value for the fibrinogen dose-dependence profile ($ED_{50}$ = 0.74 nM) was approximately double the corresponding value for the albumin dose response curve ($ED_{50}$ = 0.32 nM). This result was consistent with the relationship between the $ED_{50}$ values that was observed by [1] for fibrinogen and albumin secretion. Given that measurements by [1] represent an independent data set that was not used for parameter estimation, the agreement between model predictions and the published dose response curves provided additional validation of the model.

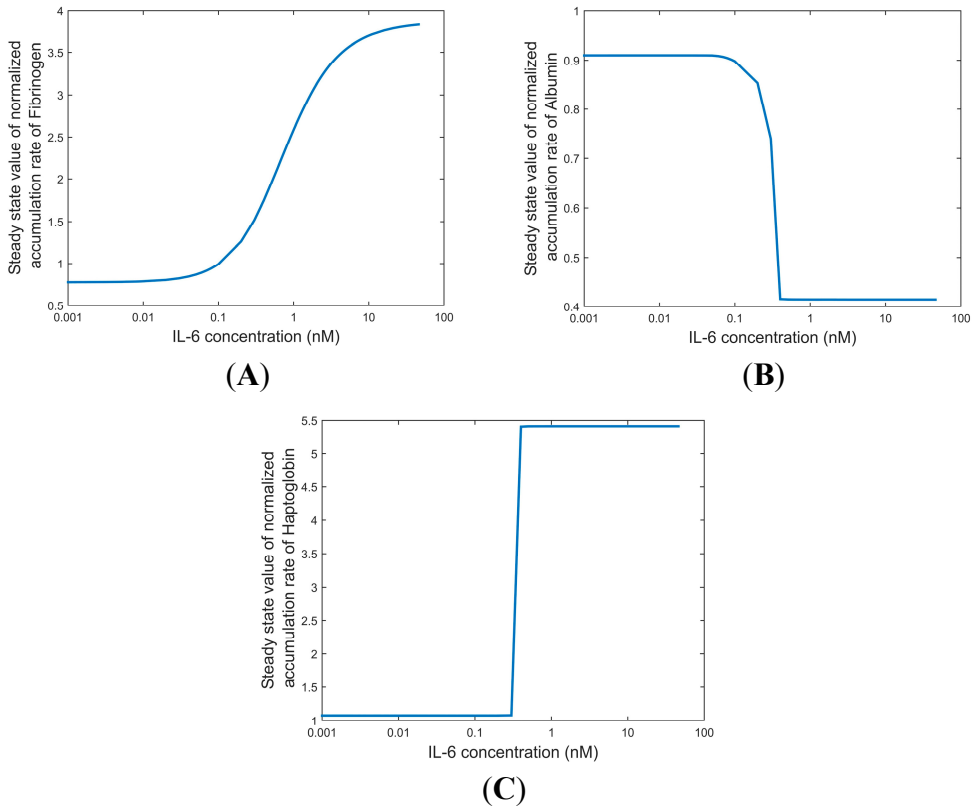


**Figure 5.** Predicted steady state values of secretion rates of fibrinogen, albumin, and haptoglobin under various stimulation doses of Interleukin-6 (IL-6): (**A**) Steady state values of secretion rates of fibrinogen; (**B**) Steady state values of secretion rates of albumin; (**C**) Steady state values of secretion rates of haptoglobin.

## 3. Investigation of Influence from the Reactions in IL-6 Signaling on the Expression Dynamics of Haptoglobin, Fibrinogen, and Albumin

In this section, sensitivity analysis was conducted to identify the reactions in the IL-6 signaling pathways that play an important role in the regulation of the expression dynamics of haptoglobin, fibrinogen, and albumin. Molecular components involved in these reactions were regarded as potential drug targets that will be further screened in Section 4.

The sensitivity analysis followed the approach of [22], in which parameters were varied by one order of magnitude above and below their nominal values. A sensitivity metric, $s_{i,j}$, was then quantified by Equation (11), in which the partial derivative of the output $y_j$ with respect to parameter $p_i$ (*i.e.*, a reaction rate constant) was normalized by the nominal values of $p_i$ and $y_j$ (*i.e.*, $p_i^0$ and $y_j^0$ respectively);

$$s_{i,j} = \frac{p_i^0 \partial y_j}{y_j^0 \partial p_i}\Big|_{\mathbf{P}_0} \tag{11}$$

where the vector $\mathbf{P}_0$ is a vector of nominal values of all parameters in the model. In this work, the output of the system, *i.e.*, $y_j$ in Equation (11), was set to the seven-day mean value of the secretion rate of haptoglobin, fibrinogen, and albumin, respectively for $j$ equal to 1, 2, and 3.

To identify the most important parameters for modeling the expression dynamics of each acute phase protein, the absolute value of $s_{i,j}$ was ranked in a decreasing order (listed in Table 1, only the top 20 parameters are listed).

As shown in Table 1, the parameters with the highest sensitivity measure values were primarily associated with those newly added reaction equations given by Equations (2) through (9) that described transcription, translation and secretion of haptoglobin, fibrinogen, and albumin, which was expected. The purpose for conducting sensitivity analysis, however, was to determine the effect of reactions from the original IL-6 signaling pathway on regulation of the expression of acute phase proteins. This information might reveal new mechanisms that can be used to manipulate the expression dynamics of acute phase proteins. In order to identify the reactions in IL-6 signal transduction that play an important role in regulation of the secretion rates of haptoglobin, fibrinogen, and albumin, the parameters shown in Table 1 were overlaid onto IL-6 signaling reaction networks in Figure 6. As seen from Table 1, most parameters that had an important impact on the secretion rate of haptoglobin also played an important role in regulating the secretion rate of albumin. This can be explained by the fact that the expression of both haptoglobin and albumin was regulated by MAPK-C/EBPβ signaling pathway. Reactions that were essential for the regulation of the expression of both haptoglobin and albumin constituted one group in Figure 6 (marked in blue pentagons), while the key reactions for regulating the expression of fibrinogen were associated with JAK-STAT pathway (marked in red ellipses in Figure 6). In addition, three reactions were identified from Table 1 for their important role in the regulation of expression dynamics of all three acute phase proteins. They were associated with the binding of IL-6 to its receptor and the formation of the receptor complex. These reactions initiated both the JAK-STAT and MAPK-C/EBPβ pathways. They were marked in purple squares in Figure 6.

**Table 1.** Sensitivity analysis results.

| Rank, $i$ | Impact on the Secretion Rate of Haptoglobin ($j$ = 1) | | Impact on the Secretion Rate of Fibrinogen ($j$ = 2) | | Impact on the Secretion Rate of Albumin ($j$ = 3) | |
|---|---|---|---|---|---|---|
| | Parameter, $p_i$ | Sensitivity, $\|s_{i,j}\|$ | Parameter, $p_i$ | Sensitivity, $\|s_{i,j}\|$ | Parameter, $p_i$ | Sensitivity, $\|s_{i,j}\|$ |
| 1 | $V_{m\_h}$ | 7.8168 | $V_{m\_f}$ | 7.0475 | $V_{m\_a}$ | 3.7746 |
| 2 | $k_{t\text{-}h}$ | 4.0417 | $K_{m\text{-}f}$ | 3.7901 | $k_{i\_a}$ | 1.0222 |
| 3 | $K_{m\_h}$ | 3.0482 | $k_{f7}$ | 2.0167 | $K_{m\_a}$ | 1.0222 |
| 4 | $k_{f51}$ | 0.5061 | $V_{m\_24}$ | 1.8237 | $k_{d\_a}$ | 1.0221 |
| 5 | $k_{f55}$ | 0.3774 | $k_{26}$ | 1.8237 | $k_{t\_a}$ | 0.5915 |
| 6 | $k_{58}$ | 0.3091 | $k_{d31}$ | 1.8100 | $k_{f51}$ | 0.1788 |
| 7 | $k_{f71}$ | 0.0075 | $k_{f27}$ | 1.8055 | $k_{f55}$ | 0.1070 |
| 8 | $k_{r71}$ | 0.0075 | $k_{d30}$ | 1.8046 | $k_{58}$ | 0.0764 |
| 9 | $K_{m69}$ | 0.0045 | $K_{m\_24}$ | 1.7836 | $k_{r71}$ | 0.0114 |
| 10 | $V_{m69}$ | 0.0044 | $k_{t\text{-}f}$ | 1.7688 | $k_{f71}$ | 0.0114 |
| 11 | $k_{70}$ | 0.0043 | $k_{r27}$ | 1.7573 | $K_{m69}$ | 0.0068 |
| 12 | $k_{f1}$ | 0.0019 | $k_8$ | 0.9580 | $V_{m69}$ | 0.0068 |
| 13 | $k_{54}$ | 0.0011 | $k_{r7}$ | 0.9403 | $k_{70}$ | 0.0066 |
| 14 | $k_{f46}$ | 0.0011 | $k_6$ | 0.8621 | $k_{f1}$ | 0.0015 |
| 15 | $k_6$ | 0.0010 | $k_{f28}$ | 0.7990 | $k_{54}$ | 0.0011 |
| 16 | $k_{f3}$ | 0.0008 | $k_{f1}$ | 0.7675 | $k_{f66}$ | 0.0010 |
| 17 | $k_{r1}$ | 0.0008 | $k_{f3}$ | 0.7628 | $k_{f46}$ | 0.0009 |
| 18 | $k_{r3}$ | 0.0007 | $k_{r1}$ | 0.7621 | $k_{r1}$ | 0.0009 |
| 19 | $k_{r5}$ | 0.0006 | $k_{r3}$ | 0.7619 | $k_{r3}$ | 0.0009 |
| 20 | $k_{f5}$ | 0.0006 | $k_{21}$ | 0.7480 | $k_{f63}$ | 0.0008 |

Figure 6 showed that reactions which influenced the regulation of fibrinogen secretion rate were mainly involved in the binding of extracellular IL-6 to its receptor on the cell membrane, the activation of STAT3C, and the expression of SOCS3. On the other hand, reactions that were related to the activation and deactivation regulation of Raf*, the activation of MEK, ERK-PP, and nuclear C/EBPβ were important to the expression of both haptoglobin and albumin.

The information in Figure 6 was used to select putative drug targets for further evaluation. In this work, good drug targets were regarded as those participating in reactions that affect the regulation of all three acute phase proteins. In addition, they should be in monomer form, as the monomer was the basic unit to form a complex [23]. Components with non-zero initial concentrations were also given priority, as they represented existing targets that the drug can bind to. Based upon these criteria, seven drug targets were selected from those important reactions as shown in Figure 6 (specifically; gp80, JAK, gp130, STAT3C, Raf, MEK, and C/EBPβ$_i$). Components gp80, JAK, gp130 were selected as they construct the receptor complex $(\mathrm{IL6}-\mathrm{gp80}-\mathrm{gp130}-\mathrm{JAK})_2^*$ which was involved in several important reactions. The other four drug targets were either directly involved or phosphorylated in those important reactions. These seven drug targets were further evaluated in Section 4 based upon the efficacy of the interaction with their drug counterparts on regulating the dynamics of acute phase proteins.

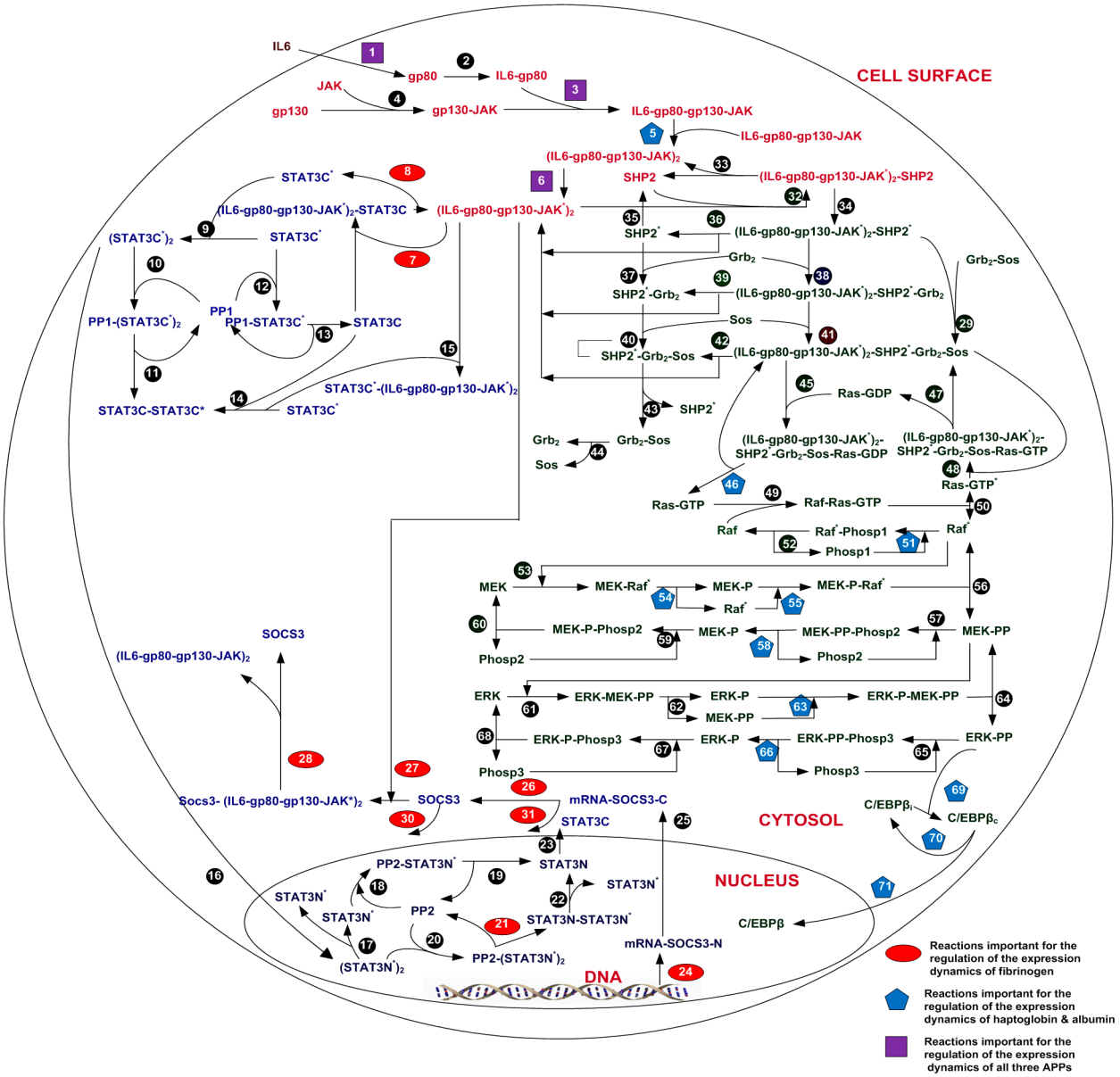


**Figure 6.** Identification of the reactions from the Interleukin-6 (IL-6) signal transduction pathway that have the largest impact on acute phase protein expression, based on results of sensitivity analysis (Table 1). The figure is adapted from [10], and the numerical labels correspond to the reaction numbering used in the model by [10]. Adapted with permission from [10]. Copyright 2011, IET.

## 4. Virtual Screening of Drug Targets and Drugs for Acute Phase Response

A good drug target should have high feasibility of binding a drug, that is, it should require low binding energy. On the other hand, the binding of a drug to a good target should cause a large influence on the dynamics of acute phase proteins. A model-based platform was developed in this section to incorporate the drug and target interaction in the extended IL-6 model to screen the seven drug targets selected in Section 3. The influence from drug binding kinetics was then investigated on the basis of the developed platform, which was followed by evaluating the treatment strategy of multiple drugs against multiple targets.

### *4.1. A Model-Based Platform to Study the Influence from the Drug (Imidazo-Pyrrolopyridine) on Acute Phase Protein Secretion*

In this work, Equation (12) was used to describe the interaction of drug and its corresponding receptor. The competitive inhibition kinetics instead of more complicated inhibition kinetics (e.g., non-competitive binding) was preferred here to elucidate the developed approach, which can be revised and extended for other inhibition kinetics.

$$\text{Target} + \text{Drug} \underset{k_f/K_i}{\overset{k_f}{\longleftrightarrow}} \text{Complex} \tag{12}$$

In Equation (12) $K_i$ was the equilibrium constant, $k_f$ was the forward rate constant, and $k_f/K_i$ was the backward rate constant. The value of $K_i$ for a drug-target pair can be obtained from experiment or computational interpretation [24]. In order to quantify the influence from the drug on the signaling pathway and thus the system output, differential equations for the drug and the drug-target complex were added into the ODE model. The differential equation for the receptor was modified accordingly. Among the seven drug targets identified from Section 3, JAK had been extensively studied for its interaction with existing drugs. Therefore, JAK and its drug counterpart imidazo-pyrrolopyridine were used as the example to illustrate our approach in this section. The corresponding value of $K_i$ was determined to be 2.5 $nM^{-1}$ from experiment [18]. Since no information was found for $k_f$ in the literature, a value of 0.01 $nM^{-1}\cdot s^{-1}$ was assigned to $k_f$ to study the dynamics of the three acute phase proteins upon the treatment with various doses of imidazo-pyrrolopyridine in Figure 7. The value of 0.01 $nM^{-1}\cdot s^{-M}$ was selected for $k_f$ here because a larger value didn't further change the expression dynamics of the three acute phase proteins in the simulation.

Since the EC50 of imidazo-pyrrolopyridine was 180 nM [18], the concentration of imidazo-pyrrolopyridine was increased from 0 to 240 nM in intervals of 60 nM, as shown in Figure 7. It can be seen that imidazo-pyrrolopyridine was predicted to greatly inhibit the secretion of fibrinogen, slightly inhibited the production of haptoglobin, and slightly promoted the secretion of albumin. The overall effect of this drug was to attenuate acute phase response, which was characterized by the decrease in the concentration of positive acute phase proteins (*i.e.*, fibrinogen and haptoglobin) but increase in the level of negative acute phase proteins (*i.e.*, albumin). In addition, the dose of imidazo-pyrrolopyridine had a significant influence on the production of fibrinogen especially, as a low dose (even lower than 60 nM) was able to repress most of the fibrinogen secretion. On the other hand, the production of hatoglobin and albumin did not change as much upon increasing the dose of imidazo-pyrrolopyridine, until a relatively high drug dose was applied.

The parameter $k_f$ reflected the speed of the drug binding reaction. Figure 8 showed the kinetics of fibrinogen expression for four values of $k_f$, as no experimental data were found for the $k_f$ value. Since imidazo-pyrrolopyridine had a large influence on the secretion of fibrinogen, only the result for fibrinogen was shown here to save space. It seems that a small increase in $k_f$ value from zero was able to suppress the secretion of fibrinogen significantly. When $k_f$ increased to 0.01 $nM^{-1}\cdot s^{-1}$, the binding of imidazo-pyrrolopyridine to JAK reached its saturated speed.

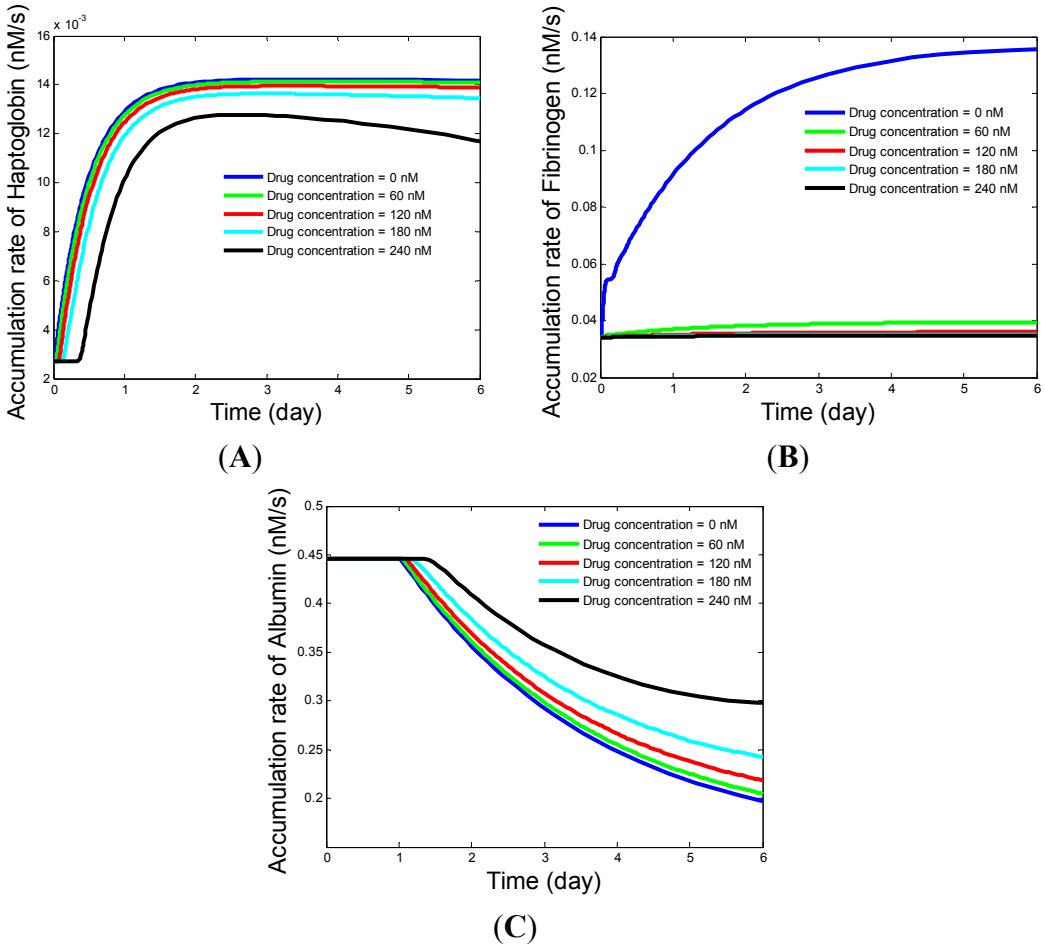


**Figure 7.** Dose effect of imidazo-pyrrolopyridine targeting at JAK on the production of three acute phase proteins: (**A**) haptoglobin; (**B**) fibrinogen; (**C**) albumin.

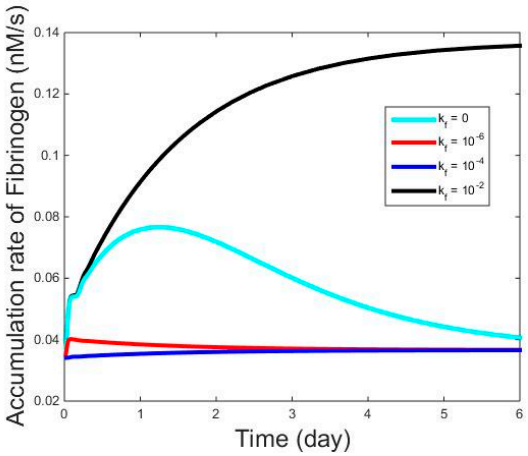


**Figure 8.** Fibrinogen expression kinetics predicted from the model with different $k_f$ values.

### *4.2. Ranking Drug Targets Based upon the Influence from Their Interaction with the Drug on the Dynamics of Acute Phase Proteins*

In this section, we further ranked the seven potential drug targets identified from Section 3 on the basis of the interaction between each drug and its target. For the same drug dose, the best drug & target

pair should return the highest effectiveness in regulating the dynamics of acute phase proteins. It was fortunate that the binding kinetics for the pair of imidazo-pyrrolopyridine and JAK was found in the literature (*i.e.*, the $K_i$ value shown in Section 4.1). However, no binding kinetic data were found for the other six drug targets identified in Section 3, although data might exist in commercial database from pharmaceutical companies (which was not accessible by public). Since the value of $K_i$ for the other six drug targets was not available in literature, it was assumed in this section that these targets were bound by the drug with the same kinetics as the one for imidazo-pyrrolopyridine and JAK. Based upon this, simulations were performed to evaluate the effectiveness of each drug-target pair on regulating the secretion rates of the three acute phase proteins. The effectiveness was quantified by the maximum percentage change in the secretion rate of each acute phase protein upon the binding of the drug to each target (Figure 9). The values of $K_i$ and $k_f$ were kept the same as those used in Section 4.1. The drug dose was set to 60 nM because the simulation result in Figure 7 implies that was a high enough concentration to suppress the fibrinogen secretion. The binding of the drug to each of gp80, JAK, and gp130 reduced the secretion rates of fibrinogen (by 74.4%, 71.0%, and 71.8%) and haptoglobin (by 44.5%, 4.2%, and 5.3%) but enhanced the production rate of albumin (by 22.9%, 1.7%, and 2.2%). The interaction from these drug-target pairs generally inhibited the acute phase response, especially in suppressing the secretion of fibrinogen. This can be explained by the fact that these three receptors played an important role in initiating both JAK-STAT and MAPK-C/EBPβ pathways. The binding of a drug to STATC inhibited the expression of fibrinogen (by 2.6%), slightly enhanced the section of haptoglobin (by 0.01%), and barely reduced the expression of albumin (by 0.006%). This made sense, as inhibition of STAT3C prevented the activation of nuclear STAT3 dimer and thus down-regulated the expression of fibrinogen. The deactivation of JAK-STAT pathway released some $(\mathrm{IL6-gp80-gp130-JAK})_2^*$ complex to MAPK-C/EBPβ pathway for enhancing the production of haptoglobin. Therefore, the drug-STAT3C interaction only partially suppressed the acute phase response. The binding of the drug to Raf and C/EBPβi enhanced the secretion rate of albumin (by 0.08% and 54.2%), but reduced the secretion rate of haptoglobin (by 0.5% and 72.6%). Since Raf and C/EBPβi were the upstream components for the activation of nuclear C/EBPβ, inhibition of these two components by drugs down-regulated haptoglobin expression and restored albumin activation. The drugs binding to either Raf or C/EBPβi only partially inhibited the acute phase response, as the secretion of fibrinogen was enhanced by 0.2% and 0.001% upon the drug binding. The drug-MEK pair showed similar effect on acute phase response as the drug-Raf or drug-C/EBPβi pair, however, the effect from the drug-MEK pair was very limited (less than 0.001%). One potential reason for this was that the initial concentration of MEK (*i.e.*, 41,667 nM) overwhelmed the drug dose (*i.e.*, 60 nM) in this simulation.

Based upon the simulation result shown in Figure 9, components gp80, gp130, and JAK were ranked as the top three drug targets because: (1) they had a noticeable effect on the secretion rates of all three acute phase proteins; and (2) they counteracted the acute phase response, while the others only partially do so. While it was assumed that the same $K_i$ was used for all the drugs in this study for screening drug targets, this assumption can be relaxed if kinetic data are available in the future.

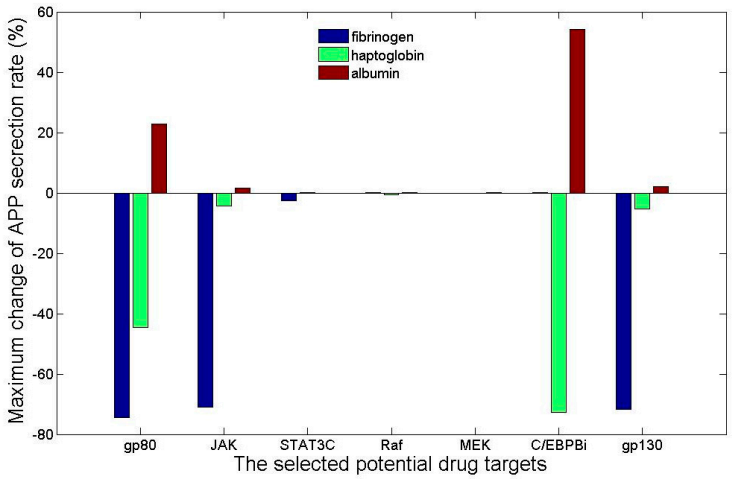


**Figure 9.** Maximum change of the secretion rates of the three acute phase proteins upon the binding of a drug with the concentration of 60 nM to each of the selected seven drug targets.

### *4.3. Influence of Multiple Drug Treatment on Acute Phase Protein Secretion*

Only single drug-target pair was studied in Sections 4.1 and 4.2. We further applied the developed platform to quantify the effectiveness of a cocktail of drugs in regulating the dynamics of acute phase proteins. Since gp80, JAK, and gp130 were identified as good drug targets for regulating acute phase proteins, they constructed the drug target pool in this study. Similar to Section 4.2, a drug with similar binding kinetics was assumed for each of these three targets, and the corresponding drug and target binding reactions (e.g., Equation (12)) were added into the extended IL-6 ODE model. The production rate of fibrinogen for the cell treated with single drug that binds to gp80, JAK, and gp130 respectively was compared to the fibrinogen production rate in the cell treated with the three drugs that aim at gp80, JAK, and gp130 respectively in Figure 10. A low dose (*i.e.*, 10 nM), was used here for each drug in all these scenarios to prove that the same effectiveness could be obtained using low doses of drugs if multiple drugs were applied to multiple drug targets. As shown in Figure 10, treating the cell with multiple drugs against multiple targets was able to enhance the inhibition of fibrinogen accumulation (see the black curve in Figure 10). Compared to the effectiveness shown in Figure 7B where 60 nM imidazo-pyrrolopyridine was applied to its target (*i.e.*, JAK), the cocktail with three drugs returned a better performance in suppressing the secretion of fibrinogen even with a lower dose (*i.e.*, 10 nM). In case that 60 nM imidazo-pyrrolopyridine might cause side effect, it was possible to get the same inhibition effectiveness by reducing its dose by adding the drugs aimed at gp80 and gp130. The developed platform can thus be used as a tool to optimize the drug cocktail if the kinetic data and side effect information are available for drug candidates, and to provide a new strategy in future drug design for acute phase response.

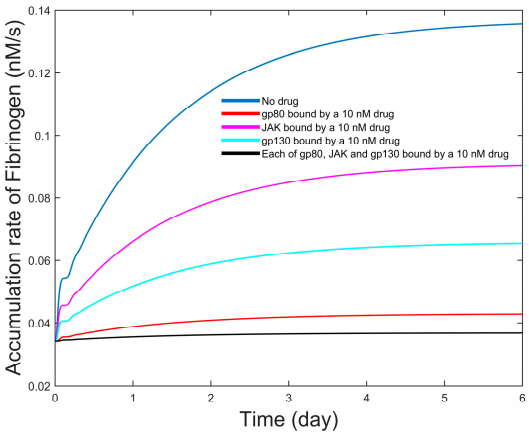


**Figure 10.** The accumulation rates of fibrinogen in the cell with only one of gp80, JAK, and gp130 bound by a single drug (10 nM) and in the cell with all gp80, JAK, gp130 bound by their drugs (each drug is of a 10 nM dose).

## 5. Discussion

This work presents the first comprehensive mathematical model for quantifying the kinetics of acute phase protein expression in the acute phase response mediated by IL-6. In addition to IL-6, it is possible for acute phase protein expression to be regulated by other cytokines, such as IL-1, TNF-α, IL-11, and OSM (oncostatin M) [25]. Although adding the signaling pathways associated with these cytokines can provide a more comprehensive model of the acute phase response, it would be a challenging task currently due to the following two reasons: (1) not all the reactions and pathways that connect these cytokines to acute phase proteins are known; (2) limited quantitative data are available for acute phase protein expression in cells stimulated by these cytokines. Therefore, we have focused on the IL-6 signaling pathway in this work. The extended IL-6 model will serve as a good starting point for incorporating other signaling pathways in the future, if quantitative data become available for acute phase protein expression following stimulation by other cytokines.

The presented IL-6 model was validated by two independent datasets that included measurements of three representative acute phase proteins for various stimulation patterns of IL-6. In addition, the dynamics of these three acute phase proteins were predicted for hepatic cells treated by single or multiple drugs. Although extensive literature review has been conducted, limited quantitative data were found to validate the predicted effects of drug treatment. Experimental research is therefore needed to further quantify the dynamics of acute phase proteins in hepatocyte cells treated with drugs targeting gp80, gp130, and JAK. Despite of this, the model is able to provide a general direction for drug target selection. For example, the model can rank potential drug targets based upon the predicted effect of the binding of a drug to each of these targets (as shown in Figure 9). With the same binding kinetics assumed for all target-drug pairs, the simulation result could reveal which drug targets, upon the competitive inhibition, have a relatively large influence on the kinetics of acute phase proteins. Since no binding affinity information is available and thus incorporated in the model, the ranking of drug targets may not completely accurate. However, the model dose provides a platform to qualitatively compare those potential drug targets. In addition, the model can be used to predict the dose response for each drug target (as shown in Figure 7 for JAK), which provides information on the

sensitivity of a drug target to the drug dose. This provides additional information for drug target screening and drug dosage selection. Furthermore, the model is able to predict the effect of the drug on the kinetics of the molecules other than the three acute phase proteins. This may be helpful to quantify the side effect of the drug.

JAK, gp80, gp130 were predicted to be the three optimal drug targets for regulating the dynamics of the acute phase proteins (*i.e.*, fibrinogen, haptoglobin, and albumin) investigated in this work. Since these three macromolecules have distinct binding sites, they can be considered as separate drug targets. Seven potential drug targets were ranked according to the influence of their interaction with drugs on the dynamics of all three acute phase proteins. In the extended IL-6 model, fibrinogen is mainly regulated by the JAK-STAT pathway while albumin and haptoglobin are associated with the MAPK pathway. Because JAK, gp80, and gp130 are involved in reactions for activating both the JAK-STAT and MAPK pathways, they were found to be better intervention points than the other four drug targets. If we aim to regulate only one or two acute phase proteins, other drug target may be better than JAK, gp80, and gp130. For example, C/EBPβi is a better drug target than JAK, gp80, and gp130 for regulating the dynamics of albumin (see Figure 9).

## 6. Conclusions

This work developed the first comprehensive IL-6 model that can predict the expression dynamics of haptoglobin, fibrinogen, and albumin in HepG2 cultures stimulated by IL-6. The developed model was validated by two different sets of experimental data, and the relative errors of the model predictions for most cases were at, or below, 15%. Based on the developed model, sensitivity analysis was conducted to identify potential drug targets for regulating acute phase protein dynamics, which included gp80, JAK, gp130, STAT3C, Raf, MEK, and C/EBP$\beta_i$. Imidazo-pyrrolopyridine targeted at JAK was used as an example drug to illustrate an approach in which the drug-target interaction is integrated with kinetic models to study the drug dose response. The simulation result showed that imidazo-pyrrolopyridine inhibited the acute phase response, especially the secretion of fibrinogen. The developed approach was used to further rank seven drug targets, with the assumption that each of them was targeted by a drug with similar binding kinetics. This assumption can be removed in the future when drug binding kinetic data are available for all drug targets. Upon binding to the drug, the targets gp80, JAK, and gp130 were found to have the largest effect on regulating the secretion of fibrinogen and on attenuating acute phase response. The developed platform was then applied to investigate the effectiveness of the drugs that bind to these three most effective targets on the regulation of fibrinogen. The simulation results show that the multiple-drug treatment approach can reduce the drug dosage to obtain the same treatment effectiveness when compared to single drug treatment approaches.

## Acknowledgments

Z.H. was supported by Villanova University (grant SRF-RSG 217030-7252; VCASE seed grants 420492 and 420265). We appreciate Noelle Comolli's help in polishing the manuscript.

## Author Contributions

Z.X. and Z.H. developed the ODE model, performed parameter estimation and sensitivity analysis. Z.X. proposed the virtual drug-screening framework. J.O.M.K. contributed to model development and sensitivity analysis, as well as interpretation of experimental data. All authors participated in the analysis of results and the preparation of the manuscript.

## Appendix

Equations added to IL-6 signal transduction for predicting dynamics of extracellular haptoglobin, fibrinogen, and albumin are shown in Equations (A1)–(A7).

$$\frac{dC_{\text{mRNA-haptoglobin}}}{dt} = \frac{V_{m\_h} C_{\text{C/EBP}\beta}}{K_{m\_h} + C_{\text{C/EBP}\beta}} - k_{t\_h} C_{\text{mRNA-haptoglobin}} \quad \text{(A1)}$$

$$\frac{dC_{\text{ex-haptoglobin}}}{dt} = r_{h0} + k_{t\_h} C_{\text{mRNA-haptoglobin}} \quad \text{(A2)}$$

$$\frac{dC_{\text{mRNA-fibrinogen}}}{dt} = \frac{V_{m\_f} C_{\text{STAT3N}^*\text{-STAT3N}^*}}{K_{m\_f} + C_{\text{STAT3N}^*\text{-STAT3N}^*}} - k_{t\_f} C_{\text{mRNA-fibrinogen}} \quad \text{(A3)}$$

$$\frac{dC_{\text{ex-fibrinogen}}}{dt} = r_{f0} + k_{t\_f} C_{\text{mRNA-fibrinogen}} \quad \text{(A4)}$$

$$\frac{dC_{\text{C/EBP}\alpha}}{dt} = -k_{i\_a} C_{\text{C/EBP}\beta} - k_{d\_a} C_{\text{C/EBP}\alpha} \quad \text{(A5)}$$

$$\frac{dC_{\text{mRNA-albumin}}}{dt} = \frac{V_{m\_a} C_{\text{C/EBP}\alpha}(t - 3600\times 24)}{K_{m\_a} + C_{\text{C/EBP}\alpha}(t - 3600\times 24)} - k_{t\_a} C_{\text{mRNA-albumin}} \quad \text{(A6)}$$

$$\frac{dC_{\text{ex-albumin}}}{dt} = r_{a0} + k_{t\_a} C_{\text{mRNA-albumin}} \quad \text{(A7)}$$

where all variables are deviation variables that represent the concentration deviations from their nominal values once HepG2 cells are stimulated by IL-6. The initial values of all these variables are thus 0 nM. Constants $r_{h0}$, $r_{f0}$, and $r_{a0}$ are the initial secretion rates of haptoglobin, fibrinogen, and albumin, respectively. Their values are determined to be 0.0027, 0.0341, and 0.4463 nM/s, from the experimental data for non-stimulated HepG2 cells. These reactions are integrated into the IL-6 signaling model presented in Moya *et al.* [10], to predict the expression dynamics of haptoglobin, fibrinogen, and albumin. The values of parameters from Equations (A1) to (A7) are listed in the following table.

**Table A1.** Values of the parameters from Equations (A1) to (A7).

| Name | Value | Unit |
|---|---|---|
| $V_{m\_h}$ | 0.06457 | nM/s |
| $K_{m\_h}$ | 99.7421 | nM |
| $k_{t\_h}$ | $2.5389 \times 10^{-5}$ | 1/s |
| $V_{m\_f}$ | 1.1841 | nM/s |
| $K_{m\_f}$ | 58.1310 | nM |
| $k_{t\_f}$ | $7.8158 \times 10^{-6}$ | 1/s |
| $k_{i\_a}$ | $1.0861 \times 10^{-3}$ | 1/s |
| $k_{d\_a}$ | 0.06866 | 1/s |
| $V_{m\_a}$ | 0.1470 | nM/s |
| $K_{m\_a}$ | 0.5118 | nM |
| $k_{t\_a}$ | $4.2195 \times 10^{-6}$ | 1/s |

## Conflicts of Interest

The authors declare no conflict of interest.

## References


1. Heinrich, P.C.; Castell, J.V.; Andus, T. Interleukin-6 and the acute phase response. *Biochem. J.* **1990**, *2653*, 621–636.
2. Heinrich, P.C.; Behrmann, I.; Haan, S.; Hermanns, H.M.; Müller-Newen, G.; Schaper, F. Principles of interleukin (IL)-6-type cytokine signalling and its regulation. *Biochem. J.* **2003**, *374*, 1–20.
3. Akira, S. IL-6-regulated transcription factors. *Int. J. Biochem. Cell Biol.* **1997**, *29*, 1401–1418.
4. Schindler, C.; Darnell, J.E., Jr. Transcriptional responses to polypeptide ligands: The JAK-STAT pathway. *Annu. Rev. Biochem.* **1995**, *64*, 621–651.
5. Yamada, S.; Shiono, S.; Joo, A.; Yoshimura, A. Control mechanism of JAK/STAT signal transduction pathway. *FEBS Lett.* **2003**, *534*, 190–196.
6. Kholodenko, B.N.; Demin, O.V.; Moehren, G.; Hoek, J.B. Quantification of short term signaling by the epidermal growth factor receptor. *J. Biol. Chem.* **1999**, *274*, 30169–30181.
7. Brightman, F.A.; Fell, D.A. Differential feedback regulation of the MAPK cascade underlies the quantitative differences in EGF and NGF signalling in PC12 cells. *FEBS Lett.* **2000**, *482*, 169–174.
8. Schoeberl, B.; Eichler-Jonsson, C.; Gilles, E.D.; Müller, G. Computational modeling of the dynamics of the MAP kinase cascade activated by surface and internalized EGF receptors. *Nat. Biotechnol.* **2002**, *20*, 370–375.
9. Singh, A.; Jayaraman, A.; Hahn, J. Modeling regulatory mechanisms in IL-6 signal transduction in hepatocytes. *Biotechnol. Bioeng.* **2006**, *95*, 850–862.
10. Moya, C.; Huang, Z.; Cheng, P.; Jayaraman, A.; Hahn, J. Investigation of IL-6 and IL-10 signalling via mathematical modelling. *IET Syst. Biol.* **2011**, *5*, 15–26.
11. Ryll, A.; Samaga, R.; Schaper, F.; Alexopoulos, L.G.; Klamt, S. Large-scale network models of IL-1 and IL-6 signalling and their hepatocellular specification. *Mol. Biosyst.* **2011**, *7*, 3253–3270.

12. Karlsson, J.O.M.; Yarmush, M.L.; Toner, M. Interaction between heat shock and interleukin 6 stimulation in the acute-phase response of human hepatoma (HepG2) cells. *Hepatology* **1998**, *28*, 994–1004.
13. Araujo, R.P.; Petricoin, E.F.; Liotta, L.A. A mathematical model of combination therapy using the EGFR signaling network. *Biosystems* **2005**, *80*, 57–69.
14. Yang, K.; Bai, H.; Ouyang, Q.; Lai, L.; Tang, C. Finding multiple target optimal intervention in disease-related molecular network. *Mol. Syst. Biol.* **2008**, *4*, 228.
15. Stump, K.L.; Lu, L.D.; Dobrzanski, P.; Serdikoff, C.; Gingrich, D.E.; Dugan, B.J.; Angeles, T.S.; Albom, M.S.; Ator, M.A.; Dorsey, B.D.; *et al*. A highly selective, orally active inhibitor of Janus kinase 2, CEP-33779, ablates disease in two mouse models of rheumatoid arthritis. *Arthritis Res. Ther.* **2011**, *13*, R68.
16. Quintás-Cardama, A.; Kantarjian, H.; Cortes, J.; Verstovsek, S. Janus kinase inhibitors for the treatment of myeloproliferative neoplasias and beyond. *Nat. Rev. Drug Discov.* **2011**, *10*, 318.
17. Kremer, J.M.; Bloom, B.J.; Breedveld, F.C.; Coombs, J.H.; Fletcher, M.P.; Gruben, D.; Krishnaswami, S.; Burgos-Vargas, R.; Wilkinson, B.; Zerbini, C.A.; *et al*. The Safety and Efficacy of a JAK Inhibitor in Patients With Active Rheumatoid Arthritis Results of a Double-Blind, Placebo-Controlled Phase IIa Trial of Three Dosage Levels of CP-690,550 Versus Placebo. *Arthritis Rheum.* **2009**, *60*, 1895–1905.
18. Hurley, C.A.; Blair, W.S.; Bull, R.J.; Chang, C.; Crackett, P.H.; Deshmukh, G.; Dyke, H.J.; Fong, R.; Ghilardi, N.; Gibbons, P.; *et al*. Novel triazolo-pyrrolopyridines as inhibitors of Janus kinase 1. *Bioorg. Med. Chem. Lett.* **2013**, *23*, 3592–3598.
19. Alam, T.; An, M.R.; Papaconstantinou, J. Differential expression of three C/EBP isoforms in multiple tissues during the acute phase response. *J. Biol. Chem.* **1992**, *267*, 5021–5024.
20. Zhang, Z.; Fuller, G.M. Interleukin 1beta inhibits interleukin 6-mediated rat gamma fibrinogen gene expression. *Blood* **2000**, *96*, 3466–3472.
21. Ruminy, P.; Gangneux, C.; Claeyssens, S.; Scotte, M.; Daveau, M.; Salier, J.P. Gene transcription in hepatocytes during the acute phase of a systemic inflammation: From transcription factors to target genes. *Inflamm. Res.* **2001**, *50*, 383–390.
22. Huang, Z.Y.; Chu, Y.F.; Hahn, J. Model simplification procedure for signal transduction pathway models: An application to IL-6 signaling. *Chem. Eng. Sci.* **2010**, *65*, 1964–1975.
23. Marianayagam, N.J.; Sunde, M.; Matthews, J.M. The power of two: Protein dimerization in biology. *Trends Biochem. Sci.* **2004**, *29*, 618–625.
24. Swanson, J.M.; Henchman, R.H.; McCammon, J.A. Revisiting free energy calculations: A theoretical connection to MM/PBSA and direct calculation of the association free energy. *Biophys. J.* **2004**, *86*, 67–74.
25. Moshage, H. Cytokines and the hepatic acute phase response. *J. Pathol.* **1997**, *181*, 257–266.